Localization in thin films of Bi with magnetic overlayers

A. K. Meikap
Indian Association for the Cultivation of Science, Materials Science Department, Calcutta 700032, India

S. K. De
Department of Physics, Visva-Bharati University, Santiniketan 731235, West Bengal, India

S. Chatterjee
Indian Association for the Cultivation of Science, Materials Science Department, Calcutta 700032, India
(Received 13 September 1991; revised manuscript received 18 May 1993)

We report the results of a comprehensive study of localization and electron-electron interaction effects in thin Bi films, Bi/Co multilayers, and Bi/Co/Bi sandwiches. Measurements of the electrical resistance and magnetoconductance have allowed us to separate the contributions to the resistance due to localization and electron-electron interactions. These have been utilized to determine the different scattering times due to these interactions. The overall behavior of these scattering times, excepting the magnetic scattering, is in good agreement with theory. Inelastic scattering has been shown to arise due to electron-electron scattering and the absolute magnitude of this scattering rate agrees reasonably well with theory. An anomalously sharp decrease of the magnetic scattering with a lowering of the temperature is observed. An explanation of this behavior has been attempted through the spin-wave theory of thin films. The observed surface magnetic impurities behave quite differently from the bulk impurities in metals and constitutes an important finding of this work.

I. INTRODUCTION

During the last decade, both theoretical[1–4] and experimental[5–9] investigations of the low-temperature electrical resistivity of weakly disordered electronic systems have led to quantum corrections to the classical Boltzmann contribution. The corrections become more and more important as the temperature approaches zero and as the amount of disorder increases. For two-dimensional or quasi-two-dimensional systems, the electrical resistivity at low temperature increases logarithmically with decreasing temperature. This nonclassical aspect of the carrier transport has been theoretically interpreted by two distinct mechanisms, the electron-electron interaction and the weak electron localization. The electron-electron interaction is less sensitive to the magnetic field and produces a positive magnetoresistance. The weak electron localization originates from interference effects between elastically scattered partial carrier waves. At very low temperature, the influence of phase-breaking scattering events such as electron-electron and electron-phonon interactions is strongly reduced and the phase coherence is maintained over relatively long distance (~ 1 μm). Also, an externally applied magnetic field suppresses the phase coherence. As a result, we get negative magnetoresistance. So weak electron localization (WEL) phenomena are confirmed by observing the sign of the magnetoresistance. Later, the theory was extended to take into account other scattering mechanisms, namely, the spin-orbit coupling, which produces an antilocalization effect, and the scattering by magnetic impurities, which produces a saturation of the additional resistivity at low temperature. Both theoretical and experimental works on the quantum corrections to thin films have been done extensively for the last ten years.[10–17] Besides pure metals, these works are extended to introduce effects of different overlayers of other metals such as Au and Pb on top of the parent metal to study the strong spin-orbit scattering[18] introduced by overlayers. These overlayers did not include magnetic materials, although recently magnetic impurities of the order of 1 ppm on top of metals such as Cu, Au, etc.,[19,20] have been extensively investigated to study the surface Kondo effect, which takes multiple scattering of the conduction electrons by one magnetic impurity into account only. The question of multiple scattering of the conduction electrons by many impurities has not been taken up until now. There are also very few theories which deal with this question, but as shown by Bergmann,[5] the method of weak electron localization studies can also be a very effective tool for studying the properties of many impurity systems. Thus, by introducing overlayers and sandwiches of magnetic materials of the order of few angstroms, one can study the properties of the magnetic impurities very easily. In our previous work,[15] we have studied the effect of overlayers of magnetic metal on top of pure Al films.

Vacuum-deposited thin films of Bi show many interesting properties, depending upon the deposition condition. Garcia, Kao, and Strongin[21] have experimentally grown bismuth films (200–1400 Å) to study the thickness dependence of the resistivity, the Hall coefficient, and the transverse magnetoresistance of a single film at different substrate temperatures. The electrical resistance of bismuth and Bi/Ag bilayers with different thicknesses was studied by George and Joy[22] at high temperature to

investigate the change in resistance due to diffusion at the interface. The superconducting transition in conjunction with structural changes of amorphous vacuum-deposited thin films has been investigated by way of electrical resistance measurements and low-temperature electron diffraction.[23–25]

Komnik *et al.*[26] studied the localization effect on bismuth films (100–200 Å) for temperatures 1.4–4.2 K and magnetic fields up to 50 kOe. A similar measurement was done by Komori, Kobayashi, and Sasaki,[27] and Woerlee, Verkade, and Jansen[28] at the same time by lowering the temperature range (0.02 K $< T <$ 10 K). Finally, Beutler and Giordano[29] extended the study to one-dimensional bismuth wire at low temperature. In spite of all these studies, the effect of magnetic layers on bismuth films and bismuth sandwiches with magnetic layers has not been studied. It is undoubtedly well known that surface and interface magnetism continue to attract considerable attention because of the fact that new electronic and magnetic features are expected to arise from the breakdown of the three-dimensional crystal symmetry. In this work we propose to study the properties of bismuth thin films due to the presence of magnetic impurities on its surface. To show both the partial superconducting transition and changes due to magnetic scattering, we have taken five samples of different layers of bismuth and cobalt ranging from 100 to 300 Å for our study.

II. THEORY

At low temperature the electrical resistance of two-dimensional disordered systems is due to weak electron localization and electron-electron interaction. In the case of strong spin-orbit scattering, the temperature dependence of the sheet resistance $R_\square$, which is the resistivity ρ divided by the film thickness d of a quasi-two-dimensional system, due to localization can be written as[2]

$$\frac{\Delta R_\square(T)}{R_\square(T_0)} = \frac{e^2 p}{4\pi^2\hbar} R_\square \ln(T/T_0) , \tag{1}$$

where p is the exponent describing the temperature dependence of the inelastic scattering rate, $\tau_i^{-1} \propto T^p$, and its value depends upon the dominant inelastic scattering mechanism as well as the effective dimensionality of the scattering process.

In the presence of a magnetic field perpendicular to the plane of the film, the low-temperature magnetoconductance of two-dimensional systems due to weak localization can be written as[4]

$$\Delta\sigma_\square(H,T) = -\frac{e^2}{2\pi^2\hbar}\left[0.5\psi\left(\tfrac{1}{2}+H_3/H\right) - 1.5\psi\left(\tfrac{1}{2}+H_2/H\right) - 0.5\ln(H_3/H) + 1.5\ln(H_2/H)\right] , \tag{2}$$

where

$$H_2 = H_i + 4H_{\text{s.o.}}/3 + 2H_s/3 ,$$
$$H_3 = H_i + 2H_s , \tag{3}$$

and H_0, H_i, $H_{\text{s.o.}}$, and H_s are the elastic, inelastic, spin-orbit, and spin-spin scattering fields, and ψ is the digamma function.

The magnetoconductance of the films studied here is at temperatures T defined by $\Delta\sigma_\square(H,T) = \sigma_\square(H,T) - \sigma_\square(0,T)$. The parameters H_0, H_i, $H_{\text{s.o.}}$, and H_s on which the different scattering process are dependent are given by the relation

$$H_x = \frac{\hbar}{4eD\tau_x} , \tag{4}$$

where $x = 0$, i, s.o., and s labels the different phase-breaking scattering processes. In the above relation, D is the diffusion constant given by $D = v_F l_e/2$, where v_F is the Fermi velocity and l_e is the mean free path.

There are two electron-electron interaction contributions. One comes from an orbital effect in the magnetic field and has been discussed by Larkin,[30] Altshuler *et al.*[31] and Fukuyama.[32] The prefactor of the orbital term scales with the superconducting transition temperature of the film. Most of our samples show no prominent superconducting properties. Hence this orbital term is negligible. The second interaction contribution, arising from spin splitting of conduction-electron energies, plays the dominant role in the transport properties of our samples. Therefore two-dimensional interaction conductivity in a large and constant field H can be written as

$$\sigma_{\square,\text{int}} = \sigma_{0,\square} + \frac{e^2}{2\pi^2\hbar}(1-\tilde{F}_\sigma/4)\ln(T) , \tag{5}$$

where $\sigma_{0,\square}$ is a constant determined by fitting the experimental magnetoconductance. $\tilde{F}_\sigma$ is the two-dimensional effective electron screening constant and is related to the general screening constant F by the relation[11]

$$\tilde{F}_\sigma = 8(1+F/2)\ln(1+F/2)/F - 4 . \tag{6}$$

Altshuler *et al.*[33,34] and Lee and Ramakrishnan[11] have shown theoretically that the two-dimensional magnetoconductance due to an electron-electron interaction is negative and this becomes important at high fields and low temperatures. Thus the low-field magnetoconduction data could be fitted using only weak localization theory. The zero-field electrical resistance is interpreted by both localization and electron-electron interaction effects.

III. EXPERIMENTAL TECHNIQUES

The Bi layer, Bi/Co bilayer, and Bi/Co/Bi sandwich were prepared by evaporating puratronic Bi and Co (from Johnson Matthey Chemicals Ltd.) from a resistively heated tungsten basket and by an electron-beam gun sequentially onto chemically and ultrasonically cleaned glass microscope slides kept at liquid-nitrogen temperature. As Bi has a tendency to degradation, we gave the samples an overcoating with a layer of 500 Å-thick silicon mono-oxide on top of Bi and Bi-Co overlayers and sandwich films. This overlayer, however, arrested the degradation to a large extent and the resistance change was found to be around 1–2 % per day. All these evaporations were done under a pressure of 10^{-6} Torr without

TABLE I. Values of thickness (d), resistivity (ρ), M, mean free path (l_e), and the diffusion coefficient (D).

Sample	Thickness d (Å)	Resistivity $\rho(10^{-5}\ \Omega\,m)$	M	Mean free path l_e (Å)	Diffusion coefficient D (10^{-3} m^2/sec)
Bi	100	2.187	0.20	92.2	1.20(1.50–3.50)[a]
Bi/Co	100/15	2.402	0.13	84.0	1.10
(Bi/Co/Bi)1	100/15/100	7.268	0.33	54.0	0.71
(Bi/Co/Bi)2	50/20/50	13.110	0.18	15.4	0.20
(Bi/Co/Bi)3	125/40/125	10.866	0.43	36.1	0.47

[a]Value obtained from Ref. 26.

breaking the vacuum. To avoid any other degradation effects, we studied the properties of freshly prepared samples. The samples were typically 200–500 μm wide and 0.3–0.5 cm long. The thickness d of the films was measured by a vibrating-quartz-crystal thickness monitor during deposition. We measured the electrical resistance R with different thicknesses (d) of films in an *in situ* arrangement and the substrate was kept at liquid-nitrogen temperature. The resistivity ρ of the samples was determined from the formula $\rho = Rbd/l$, where b, d, and l are the width, thickness, and length of the samples, respectively. We observed that $\rho \propto 1/d$, and from this behavior we calculated[35] the electronic mean free path (l_e) and diffusion constant (D) as shown in Table I. The low-temperature measurements[14] were performed using a ^{4}He cryostat equipped with an 8-T Nb-Ti superconducting magnet. The sample resistance was measured by applying the standard four-terminal voltage technique, using both a Hewlett-Packard 3468B digital multimeter and a Keithley 220 programmable current source coupled to a nanovoltmeter.

The thickness of the films is more important in order to study the localization effects. The films are considered as two dimensional with respect to weak localization when the diffusion time from the top of the film to the bottom is small in comparison to the characteristic time of the electrons.[10] In zero magnetic field, the characteristic time is the inelastic scattering time of the conduction electrons; the films are two dimensional with respect to weak localization when the inelastic length $l_i = (D\tau_i)^{1/2}$ is much greater than the film thickness d, i.e., $(D\tau_i)^{1/2} \gg d$. But in the presence of a magnetic field, the characteristic time is given by $\tau_H = \hbar/(4eDH)$; thus, the condition of two dimensionality in the presence of a magnetic field is $(D\tau_H)^{1/2} \gg d$. This restriction limits the two-dimensional region of the magnetoconductance data to $H \ll 4.8$ T for Bi, Bi/Co, and (Bi/Co/Bi)2, $H \ll 1.3$ T for (Bi/Co/Bi)1, and $H \ll 0.73$ T for (Bi/Co/Bi)3 films. For the electron-electron interaction, the characteristic time is $\tau_T = \hbar/(2\pi K_B T)$. Therefore a thin film is two dimensional when $(D\tau_T)^{1/2} \gg d$. These criteria are satisfied for a temperature $T \ll 14.6$ K for Bi, $T \ll 9.2$ K for Bi/Co, and $T \ll 2$ K for Bi/Co/Bi systems.

IV. RESULTS AND DISCUSSION

We have measured the electrical resistance in the absence and presence of the perpendicular magnetic field of several samples in the temperature range $1.9\ \text{K} \leq T \leq 300$ K. At high temperatures the electrical resistivity decreases with increasing temperature, i.e., semiconducting behavior. This behavior at higher temperature is consistent with previous works[21,27,28] on Bi. But there is a peculiar behavior in the low-temperature resistance. Figure 1 represents the variation of the electrical resistance with temperature for the different samples. From Fig. 1 it is seen that the samples of thickness around 100 Å show a transition in resistivity (6–8 % of its original value) around 3–5 K. This change is not observed in (Bi/Co/Bi)1 and (Bi/Co/Bi)3 samples. This transition is destroyed by applying a magnetic field as shown in Fig. 2 for the Bi/Co sample. Bismuth in the crystalline state does not show any superconducting transition down to the lowest temperature. But when bismuth is taken in the amorphous state, it shows superconductivity.[23–25] The amorphous state is usually obtained by depositing Bi by the evaporation technique on the substrate usually held at low temperature, i.e., lower than the crystallization temperature. This crystallization temperature becomes higher if the film thickness decreases. For films with a thickness of about 100 Å, the crystallization temperature is usually in the liquid-nitrogen temperature

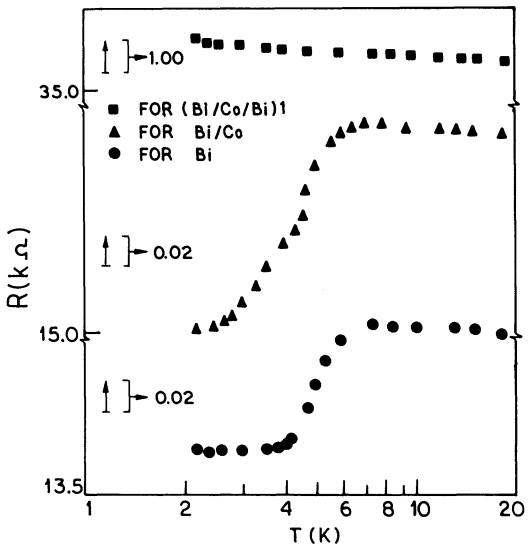

FIG. 1. Resistance as a function of temperature for different films.

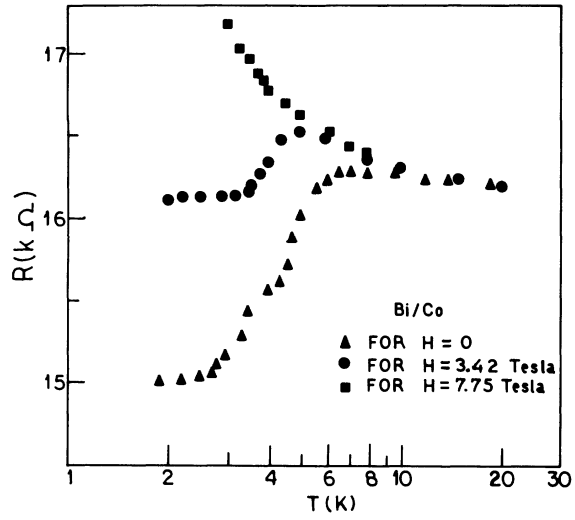

FIG. 2. Resistance as a function of temperature for several values of the magnetic field, for a 115-Å-thick Bi/Co film with 100 Å Bi and 15 Å Co.

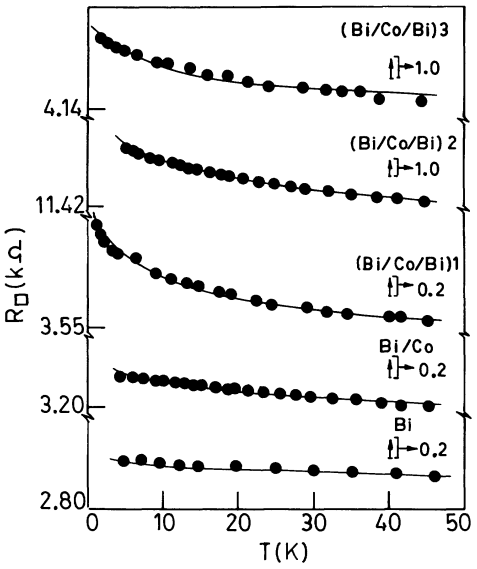

FIG. 3. Sheet resistance ($R_\square$) vs temperature for the five samples. Different points are the experimental data. Solid lines represent a least-squares fit of data points to the ln(T) dependence.

range. Moreover, by lowering the degree of vacuum or the deposition rate, the crystallization temperature is increased considerably. We have deposited our films on a glass substrate kept at liquid-nitrogen temperature under a vacuum (10^{-6} Torr) at the very slow rate of 0.3–0.5 Å/sec. As a result, we expect the films of thickness around 100 Å to show an amorphous phase, whereas films of thickness $d > 200$ Å show only the crystalline as a result of their crystallization temperature being lower than the substrate temperature. Thus the partial superconducting transition observed in our samples is probably due to the local presence of amorphous regions. The comparatively thicker (Bi/Co/Bi)1 and (Bi/Co/Bi)3 films in our case do not contain the residual amorphous phase. As a result, we do not observe any resistivity transition in the temperature region $1.9\ \text{K} \leq T \leq 300\ \text{K}$.

The sheet resistance ($R_\square$) of various samples as a function of temperature is shown in Fig. 3. The $R_\square(T)$ curves are best fitted by ln(T) in the temperature range $1.9\ \text{K} \leq T \leq 50\ \text{K}$ as shown in Fig. 3. Thus our $R_\square(T)$ values are in good agreement with weak disorder theories for two-dimensional systems. This behavior is also consistent with that seen by previous workers.[26,29] In Fig. 4 we plot the fractional resistance change as a function of temperature. From the figure we observe that the temperature dependence $\Delta R(T)/R(T_0)$ for all of our samples is accurately logarithmic. Deriving the slopes $\{d[\Delta R(T)/R(T_0)]\}d(\ln T)$ of these straight lines and comparing these with Eq. (1) and the theory of Altshuler, Aronov, and Lee,[33] we have estimated the values of M $[=p/2-(1-\frac{3}{4}F)]$ as presented in Table I. Again, low-field magnetoconductance data yield apparent values of p (exponent taken from τ_i versus T curve). From these values we have calculated the screening factor F, which lies in the range $0 < F < 1$ for our samples. Thus the temperature dependence of magnetoconductance is dominated by interaction effects and by the screening factor F.

We have measured the magnetoresistance of our Bi, Bi/Co, and Bi/Co/Bi films over a wide range of field and temperature. Some typical results for conductance as a function of temperature at constant perpendicular magnetic field are shown in Fig. 5. A logarithmic variation with temperature is also seen in relatively large fields. Since such a large magnetic field quenches the effects of localization, the conductance variation seen in this case is due predominantly to interaction. The fact that the high-field behavior is logarithmic implies that the interaction effects are two dimensional with $L_T \gg d$. In Fig. 5 the points are the experimental conductance data at a magnetic field of 7.75 T and the solid lines are the best-

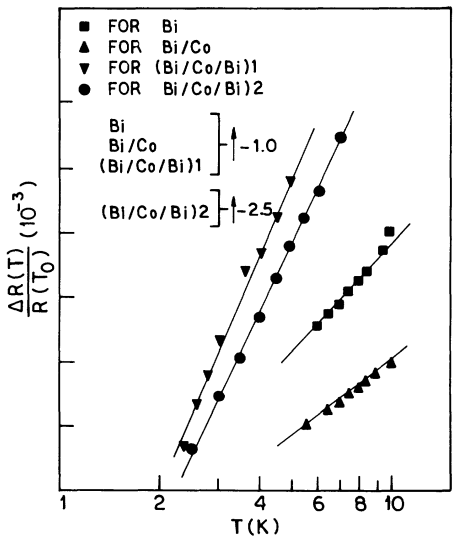

FIG. 4. Fractional change in zero-field resistance $\Delta R(T)/R(T_0)$ vs ln(T) for four samples.

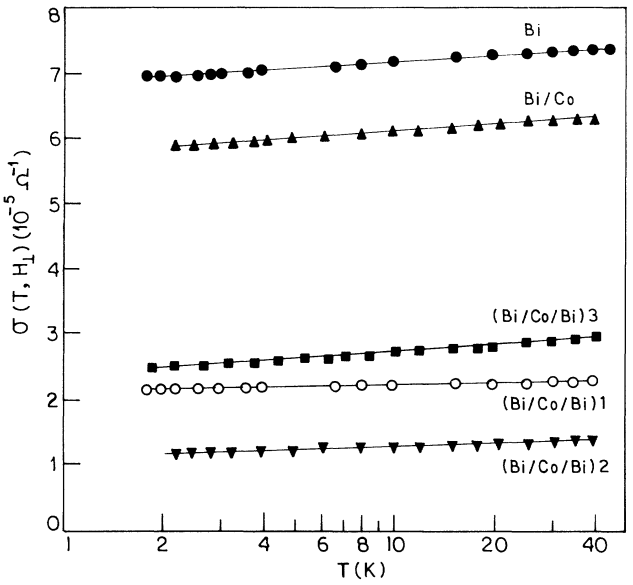

FIG. 5. Conductance as a function of temperature for a fixed magnetic field $H=7.75$ T, for different samples. The field is applied perpendicular to the plane of the film. The solid lines indicate a least-squares fit of data points to Eq. (5), which illustrate a logarithmic temperature dependence.

fitted theoretical curves obtained from Eq. (5) with $\sigma_{0,\Box}$ and $\tilde{F}_\sigma$ as the fitting parameters. The values of $\sigma_{0,\Box}$ and $\tilde{F}_\sigma$ are shown in Table II.

The perpendicular magnetoconductance at the temperature 4.2 K of the different samples is shown in Fig. 6. The magnetoconductance is always negative, as a result of the very strong spin-orbit scattering process. It is evident from the figure that the magnitude of the magnetoconductance decreases by introducing the Co layers on the surface of Bi films. This is due to the fact that the Co atoms introduce a weak spin-orbit scattering to the Bi films as a result of its lower atomic number ($Z_{Co}=27$) than Bi ($Z_{Bi}=83$). However, in (Bi/Co/Bi)1 film, the magnetoconductance is reduced more than the Bi/Co film. This is because the impurities from the Co layers, being covered by a Bi layer, are transformed into a bulk Co impurity from surface impurities[36] and as a result, the spin-orbit scattering becomes weaker. Although in the Bi/Co system the screening on the surface of Bi should be complete, it appears from the results of the Bi/Co/Bi sandwich that screening is not complete. It may be that 15 Å of Co layers is not sufficient to complete the screening. From Figs. 7 and 8 it is seen that the magnetoconductance is prominent at low temperature and its magnitude decreases with an increase of temperature. This results from the temperature dependence of the inelastic scattering time $\tau_i \propto T^{-p}$. It is also seen that the magnetoconductance at higher magnetic field is mostly saturated. This is due to the fact that at high field the spin states of the complementary waves are essentially unchanged.

Since the sign of the magnetoconductance of all our samples is negative, we have analyzed our magnetoconductance data by the theory of antilocalization and electron electron interaction (EEI). At low field and low temperature, the contribution to the magnetoconductance due to EEI is very small. So we can interpret the magnetoconductance data by the antilocalization in the low-field region. The different scattering fields H_i, H_s, and $H_{s.o.}$ enter in the magnetoconductance through two combinations as indicated by Eqs. (2) and (3). For a strong spin-orbit interaction, $H_{s.o.}$ is much greater than both H_i and H_s; hence, from Eq. (3), we have $H_2 \approx 4H_{s.o.}/3 + H_\phi/3$ and $H_\phi = H_3 = H_i + 2H_s$. Therefore, to calculate the different scattering fields, we have fitted the magnetoconductance data as a function of perpendicular magnetic field for a particular temperature using Eq. (2) with the phase scattering field ($H_\phi = H_i + 2H_s$) and spin-orbit scattering field ($H_{s.o.}$) as the fitting parameters. In a nonlinear least-squares fitting method, generally three techniques are used: (i) grid search, (ii) gradient search (method of steepest descent), and (iii) analytical Taylor-series expansion of the fitting function. Another powerful and widely used method is Marquardt's method, which can be easily implemented with the analytical method. We have used the analytical method by Taylor-series expansion of $\Delta\sigma_\Box(H,T)$ about the estimated values of H_ϕ and $H_{s.o.}$. The best-fitted values of H_ϕ and $H_{s.o.}$ are calculated independently by a least-squares fit of experimental magnetoconductance data with Eq. (2) using Marquardt's iteration technique.[37,38] In the superconducting region, magnetoconductance is affected as a result of the superconducting fluctuation. The theoretical calculation of magnetoconductance including this effect, done by Larkin,[30] gives an additional term in Eq. (2). This correction in the super-

TABLE II. Values of $\sigma_{0,\Box}$, effective electron screening constant ($\tilde{F}_\sigma$), elastic scattering time (τ_0), phase scattering time (τ_ϕ), and spin-orbit scattering time ($\tau_{s.o.}$).

Sample	$\sigma_{0,\Box}$ ($10^{-5}\ \Omega^{-1}$)	$\tilde{F}_\sigma$	τ_0 (10^{-13} sec)		τ_ϕ (10^{-11} sec) at 4.2 K		$\tau_{s.o.}$ (10^{-12} sec)	
Bi	58.07	0.20	0.355	1.900[a]	2.580	1.00[b]	0.465	0.480[a]
Bi/Co	40.06	0.36	0.323		0.221		0.512	
(Bi/Co/Bi)1	53.60	0.75	0.208		0.870		0.670	
(Bi/Co/Bi)2	17.04	0.95	0.060		0.661		1.628	
(Bi/Co/Bi)3	19.09	0.23	0.139		0.365		1.152	

[a]Values obtained from Ref. 39.
[b]Values obtained from Ref. 26.

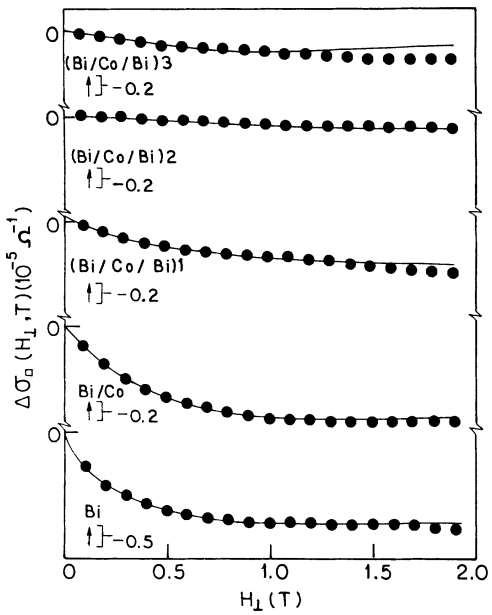

FIG. 6. Magnetoconductance curves of pure Bi and the system of Bi as the host and Co as the impurities at 4.2 K. The points represent the experimental result; the solid lines are the theoretical curves.

conducting region is prominent when the resistance drop is at least 50%, as has been done in our earlier work.[15] Since in this case (Bi/Co/Bi)1 and (Bi/Co/Bi)3 do not show any resistance drop, whereas the other samples have only a 6–8 % resistance drop, we have ignored the correction in the superconducting region for this fitting. Since our samples are spectroscopically pure, we assume

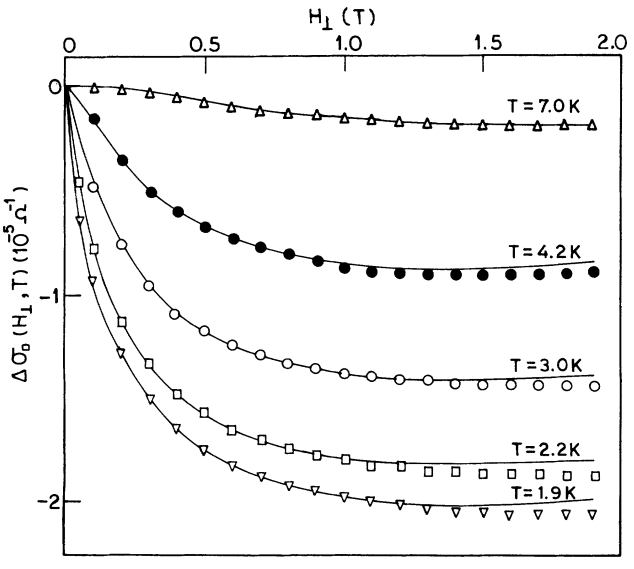

FIG. 7. Magnetoconductance data of the (Bi/Co/Bi)1 sample as a function of applied perpendicular magnetic field at different fixed temperatures. Points are measured data, and solid lines are theoretical fits to Eq. (2).

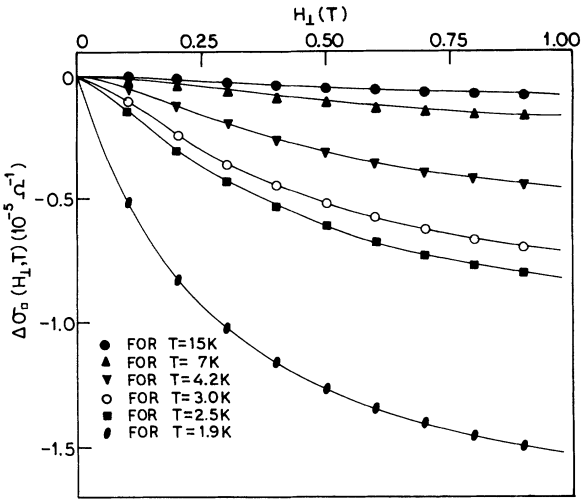

FIG. 8. Magnetoconductance data of the Bi/Co sample as a function of applied perpendicular magnetic field at different fixed temperatures. Points are measured data, and solid lines are theoretical fits to Eq. (2).

that the magnetic scattering is negligible ($H_s=0$) for the fitting of Bi films and $H_\phi=H_i$. However, in bismuth with cobalt systems, we take H_ϕ and $H_{s.o.}$ as the fitting parameters. Figures 7 and 8 show good agreement between the experimental and theoretical values of magnetoconductance. The values of different scattering times are calculated from Eq. (4) using the best-fitted values of the parameters H_ϕ and $H_{s.o.}$ and are shown in Table II. These are in good agreement with previous works.[26,39]

According to the prediction of Abrikosov and Gorkov,[40] the spin-orbit scattering depends on the atomic number (Z) of the metals through the relation $\tau_0/\tau_{s.o.}=(\beta Z)^4$, where β is the fine-structure constant. If we consider only the Bi atoms ($Z=83$) in our films, then the theoretical value is $\tau_0/\tau_{s.o.}=0.135$. But our experimental value is $\tau_0/\tau_{s.o.}=0.076$ for Bi. This small deviation arises because of the choice of Z. If the scattering is caused by vacancies, lattice defects, or are due to the metal-vacuum interface, Z should be the nuclear charge of Bi, 83. If the dominant scattering mechanism is scattering from impurities, the appropriate value for Z may be that of the impurity. However, the experimental values of $\tau_0/\tau_{s.o.}$ for Bi/Co and (Bi/Co/Bi)1 are 0.063 and 0.031, respectively. In comparison with the Bi films, the value of $\tau_0/\tau_{s.o.}$ is reduced in Bi/Co and (Bi/Co/Bi)1 films. This reduction arises because of the fact that our films contain not only Bi, but also lower-atomic-number ($Z=27$) cobalt atoms. This cobalt atom reduces the spin-orbit scattering of Bi. In (Bi/Co/Bi)1 films the reduction is more than Bi/Co; this is because the Co atoms in (Bi/Co/Bi)1 act as bulk impurities, whereas in Bi/Co they act as surface impurities.

The temperature dependence of the phase scattering field H_ϕ is shown in Fig. 9 for the Bi/Co and (Bi/Co/Bi)1 samples. The phase scattering originates due to both the inelastic scattering and the spin-spin scattering. The in-

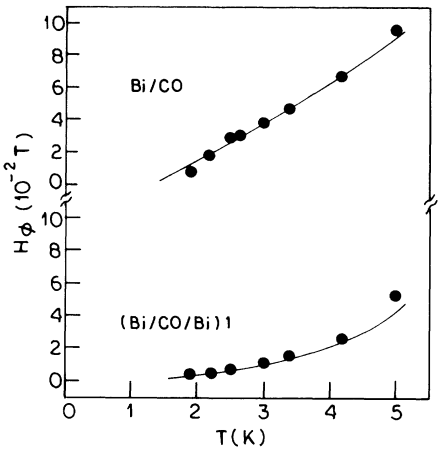

FIG. 9. Phase scattering field (H_ϕ) vs temperature (T) for different samples. Different points are the calculated values from experimental data. The solid lines represent theoretical values from Eq. (7).

elastic scattering arises as a result of two important mechanisms: One is electron-phonon ($\tau_{e\text{-}p}^{-1}$) scattering and the other is electron-electron ($\tau_{e\text{-}e}^{-1}$) scattering. On the basis of the single-particle interference picture of weak localization, Rammer and Schmid[41] have calculated the electron-phonon scattering rate ($\tau_{e\text{-}p}^{-1}$). Using the theory of Rammer and Schmid,[41] we have $\tau_{e\text{-}p}^{-1}=6.48\times10^{8}$ sec^{-1} at $T=1.9$ K for Bi. Hence this value is much smaller than the calculated values of $\tau_i^{-1}=3.79\times10^{10}$ sec^{-1} at $T=1.9$ K. Thus, in the temperature range $1.9\ K\leq T\leq5$ K, the contribution of the electron-phonon scattering is negligibly small. The standard result for the electron-electron scattering rate in clean two-dimensional systems ($T>\hbar/K_B\tau_0$) is proportional to T^2. Altshuler, Aronov, and Khmel'nitskii[42] and Eiler[43] have calculated the electron-electron scattering at small energy transfer. They also predict that the electron-electron scattering rate for two-dimensional systems [$d\ll(\hbar D/K_BT)^{1/2}$] is proportional to T, with the proportional constant A [$=(eR_\square K_B)/(8\pi\hbar D)\ln\{\pi\hbar/(e^2R_\square)\}$]. Therefore the inelastic scattering and magnetic scattering can be extracted by making the arguments based on the assumed temperature dependence of H_i and H_s. We have performed a series of least-squares fits of our results for H_ϕ by assuming the different possible temperature-dependent functions for H_s. But only the form of the following expression is best suited for H_ϕ:

$$H_\phi=AT+BT\exp(-C/T)\ , \tag{7}$$

where A, B, and C are constants which are allowed to vary to obtain a best fit. The first term in Eq.(7) on the right represents inelastic scattering, while the second term represents spin-spin scattering. The solid lines in Fig. 9 are the best-fitted line with A, B, and C equal to 3.19×10^{-3}, 3.24×10^{-2}, and 3.75, respectively, for Bi/Co and 1.76×10^{-3}, 9.92×10^{-3}, and 4.30, respectively, for (Bi/Co/Bi)1. From these temperature dependence arguments, we can separate the inelastic scattering field and spin-spin scattering field as shown in Figs. 10(a) and 10(b), respectively. We note that the theoretical values of A as predicted by Altshuler, Aronov, and Khmel'nitskii,[42] and Eiler[43] are in reasonably good agreement with our experimentally fit values. Thus the inelastic electron scattering in Bi, Bi/Co, and Bi/Co/Bi films at liquid-helium temperature is due to electron-electron scattering only.

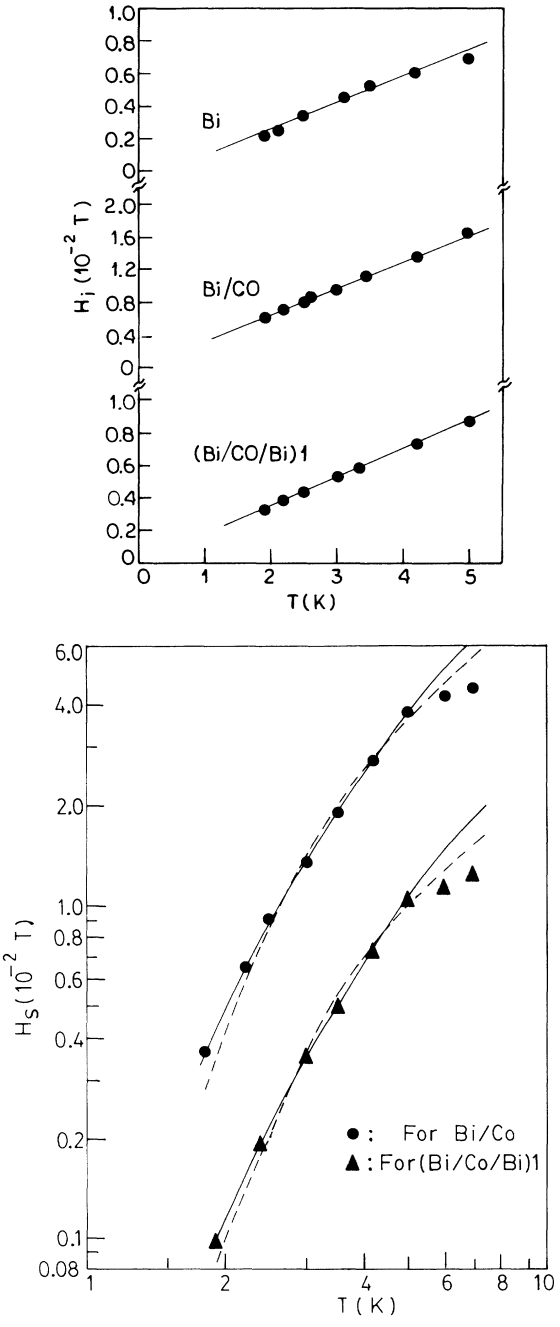

FIG. 10. (a) Temperature dependence of the inelastic scattering field in tesla of the Bi, Bi/Co, and (Bi/Co/Bi)1 samples. (b) Temperature dependence of the magnetic scattering field in tesla of the Bi/Co and (Bi/Co/Bi)1 samples along with the theoretical predictions from the crystal-field and spin-wave theory of thin films. The solid lines are due to spin-wave theory, and dashed lines are due to crystal-field splitting.

The variation of magnetic scattering field H_s with temperature T is shown in Fig. 10(b). The figure shows that the magnetic scattering appears to be almost constant above 5 K and decreases sharply as the temperature is lowered. A similar behavior of the magnetic scattering field is obtained in our previous work[15] in Al/Co and Al/Co/Al systems. Because of the presence of magnetic impurities on the surface of Bi films, one can consider the influence of crystal fields on the magnetic scattering. In this theory crystal fields destroy the degeneracy of the $(2S+1)$ states of a free atom with spin S. As a result, the magnetic scattering causing a transition between the energy levels decreases with decreasing temperature. A crystal-field splitting of Δ should result in an experimental freezing proportional to $\exp(-\Delta/K_BT)$. At high temperatures, the magnetic scattering field becomes constant. This is because at high temperature the thermal energy permits transitions between the split energy levels. The best-fitted theoretical values due to the crystal-field splitting are shown in Fig. 10(b). From this figure it is observed that the experimental magnetic scattering at low temperature cannot be explained by the above prediction. A similar effect was observed by Peters, Bergmann, and Mueller,[44] for magnetic impurities of the order of a small fraction of an atomic layer on top of Cu, Au, and Ag. They suggested a universal behavior proportional to $T^{1/2}$ for the scattering by interacting magnetic impurities. However, the magnetic scattering field of our films does not obey the above prediction because of the fact that our samples contain a larger amount of magnetic impurities. Levy and Motchane[45] suggested that in the case of continuous and island films the spin of the ferromagnetic thin films deviate from their saturation. They have also calculated the temperature dependence of the saturation magnetization $M(T)$ by thin-film spin-wave theory and have shown that there is a sharp drop of $M(T)$ at low temperature as $T\exp(-E_g/K_BT)$, where E_g is the effective anisotropy energy. We have also plotted in Fig. 10(b) the best-fitted theoretical values using the relation $H_s(T) \propto T\exp(-C/T)$. So we would expect from the two theoretical curves (crystal-field splitting+spin-wave approach) as shown in Fig. 10(b) that the sharp decrease of magnetic scattering fields (H_s) may be due to spin-wave theory at low temperature.

The most outstanding feature of the magnetoconductance data occurs in higher fields. From Fig. 7 we see that the experimental magnetoconductance is greater than the theoretical values as calculated by Eq. (2) at high fields ($H > 1$ T). This is due to the fact that the electron-electron interaction introduces an additional negative magnetoconductance at high field. In order to calculate the magnetoconductance due to the electron-electron interaction effect, we first extrapolate the magnetoconductance predictions of weak localization theory to magnetic fields higher than those used in the low-field fitting region, and second, we subtract this contribution from the experimental magnetoconductance data. These subtracted values for $\Delta\sigma_{\Box,\text{int}}$ are plotted in Figs. 11 and 12 and as a function of the dimensionless parameter $f=g\mu_BH/K_BT$. The solid lines in the figures are the theoretical curves obtained from the theory of Altshuler

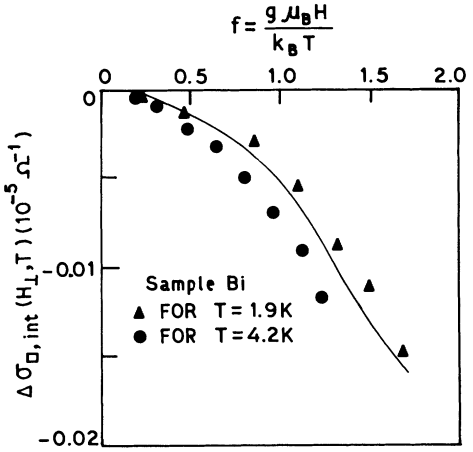

FIG. 11. Magnetoconductance due to electron-electron interaction obtained as a function of the dimensionless parameter $f=g\mu_BH/K_BT$ of a Bi film. The points are obtained by subtracting the magnetoconductance due to the weak localization predictions from the experimental data. The solid line is the theoretical values from the theory of Altshuler *et al.* (Refs. 33 and 34).

et al.[33,34] which have used the values of $\tilde{F}_\sigma$ from Table II. The figures show a deviation between experimental and theoretical values. According to the theory of Altshuler *et al.*, different combinations of T and H which give rise to the same value of f should yield the same values of $\Delta\sigma_{\Box,\text{int}}$. But experimental results do not obey this prediction. Considering the measuring accuracy in magnetoconductance data and considering the beautiful fit of these data with the theory in the low-field region ($H < 1$ T), we believe that this discrepancy cannot be due to the magnetoconductance measurements. However,

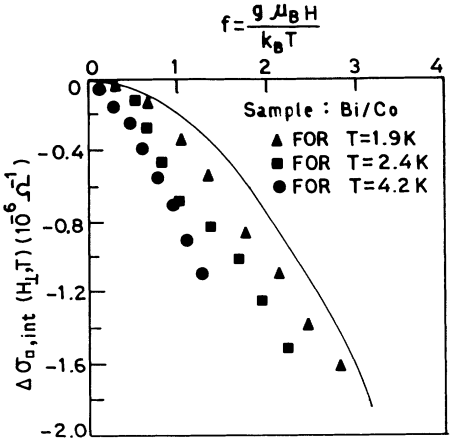

FIG. 12. Magnetoconductance due to electron-electron interaction obtained as a function of the dimensionless parameter $f=g\mu_BH/K_BT$ of a Bi/Co film. The points are obtained by subtracting the magnetoconductance predictions due to the weak electron localization from the experimental data. The solid lines are the theoretical values from the theory of Altshuler *et al.* (Refs. 33 and 34).

the figures show that the deviation between the experimental and theoretical values is less at lower temperature. So we should expect that the very-low-temperature data ($T<1$ K) will be in good agreement with the theory.[33,34] A similar result is obtained by Ben-Shlomo and Rosenbaum.[46]

V. CONCLUSION

In this work we have studied the transport properties of thin Bi, Bi/Co, and Bi/Co/Bi films at low temperatures to understand the anomalous behavior of these samples. From the magnetoconductance data, we have calculated the different scattering fields such as inelastic (H_i), spin-orbit ($H_{s.o.}$), and spin-spin (H_s) scattering fields. The spin-orbit scattering field does not depend on temperature and is greater in comparison to the inelastic and spin-spin scattering fields, suggesting an antilocalization effect to be responsible for the large $H_{s.o.}$. At low temperature, the inelastic scattering in the films is found to be due to electron-electron scattering in the presence of disorder and agrees well with the theory of this process. The spin-orbit and spin-spin scatterings are reduced as a result of the presence of bismuth over the cobalt layers. The high-temperature variation of the magnetic scattering is explained by crystal-field theory. However, the behavior of H_s at low ($T<5$ K) temperature is much more difficult to explain. A possible explanation of this behavior has been put forward through the spin-wave theory of the thin films. It appears that the present theories are not sufficient to explain the phenomena. We believe that more experimental and theoretical studies of this behavior are needed to obtain a satisfactory answer. Finally, we summarize the result of our investigation.

(1) Magnetic scattering depends on temperature and satisfies the relation $T\exp(-C/T)$ at low temperature. This finding needs more experimental and theoretical studies to understand it.

(2) The magnetoresistance due to the electron-electron interaction does not obey the theoretical prediction at temperature $T>1.9$ K. However, it may be in good agreement at very low temperature.

ACKNOWLEDGMENTS

This work has been performed under a grant by the Department of Science and Technology, Government of India. We wish to acknowledge our gratitude for this financial support during this work.

[1]D. J. Thouless, Phys. Rev. Lett. **39**, 116 (1977).
[2]E. Abrahams, P. W. Anderson, D. C. Licciardello, and T. V. Ramakrishnan, Phys. Rev. Lett. **42**, 673 (1979).
[3]P. W. Anderson, D. J. Thouless, E. Abrahams, and D. S. Figher, Phys. Rev. B **29**, 3519 (1980).
[4]S. Hikami, A. I. Larkin, and Y. Nagaoka, Prog. Theor. Phys. **63**, 707 (1980).
[5]G. Bergmann, Phys. Rev. Lett. **48**, 1048 (1982); Z. Phys. B **48**, 5 (1982).
[6]E. White, R. C. Dynes, and J. P. Garno, Phys. Rev. B **29**, 3694 (1984).
[7]F. Komori, S. Kobayashi, and W. Sasaki, J. Phys. Soc. Jpn. **51**, 3136 (1982).
[8]P. Santhanam, S. Wind, and D. E. Prober, Phys. Rev. B **35**, 3188 (1987).
[9]A. K. Meikap, A. R. Jana, S. K. De, and S. Chatterjee, Phys. Status Solidi B **160**, 473 (1990).
[10]G. Bergmann, Phys. Rep. **107**, 1 (1984).
[11]P. A. Lee and T. V. Ramakrishnan, Rev. Mod. Phys. **57**, 287 (1985).
[12]S. Chakraborty and A. Schmid, Phys. Rep. **140**, 193 (1986).
[13]L. Piraun, J. Mater. Res. **5**, 1285 (1990).
[14]A. K. Meikap, A. R. Jana, S. K. De, and S. Chatterjee, J. Low Temp. Phys. **85**, 295 (1991).
[15]A. K. Meikap, A. R. Jana, S. K. De, and S. Chatterjee, Solid State Commun. **77**, 249 (1991).
[16]D. Abraham and R. Rosenbaum, Phys. Rev. B **27**, 1413 (1983).
[17]A. C. Sacharoff and R. M. Westervelt, Phys. Rev. B **32**, 662 (1985).
[18]D. Abraham and R. Rosenbaum, J. Phys. C **17**, 2627 (1984).
[19]C. V. Haesendonck, J. Vranken, and Y. Bruynseraede, Phys. Rev. Lett. **58**, 1968 (1987).
[20]R. P. Peters, G. Bergmann, and R. M. Mueller, Phys. Rev. Lett. **58**, 1964 (1987).
[21]N. Garcia, Y. H. Kao, and M. Strongin, Phys. Rev. B **5**, 2029 (1972).
[22]J. George and E. C. Joy, Thin Solid Films **74**, 153 (1980).
[23]W. Buckel and R. Hilsch, Z. Phys. **138**, 109 (1954).
[24]N. Kurti and F. E. Simon, Proc. R. Soc. London A **151**, 610 (1935).
[25]T. Hamada, K. Yamakawa, and F. E. Fujita, J. Phys. F **11**, 657 (1981).
[26]Y. F. Komnik, E. I. Bukhshtab, V. V. Andrievskii, and A. V. Butenko, J. Low Temp. Phys. **52**, 325 (1983).
[27]F. Komori, S. Kobayashi, and W. Sasaki, J. Phys. Soc. Jpn. **52**, 4306 (1983).
[28]P. H. Woerlee, G. C. Verkade, and A. G. M. Jansen, J. Phys. C **16**, 3011 (1983).
[29]D. E. Beutler and N. Giordano, Phys. Rev. B **38**, 8 (1988).
[30]A. I. Larkin, Pis'ma Zh. Eksp. Theor. Fiz. **31**, 209 (1980) [JETP Lett. **31**, 219 (1980)].
[31]B. L. Altshuler, A. G. Aronov, D. E. Khmelnitskii, and A. I. Larkin, Zh. Eksp. Theor. Fiz. **81**, 768 (1981) [Sov. Phys. JETP **54**, 411 (1981)].
[32]H. Fukuyama, J. Phys. Soc. Jpn. **50**, 3407 (1981).
[33]B. L. Altshuler, A. G. Aronov, and P. A. Lee, Phys. Rev. Lett. **44**, 1288 (1980).
[34]E. L. Altshuler, D. Khmelnitzkii, A. I. Larkin, and P. A. Lee, Phys. Rev. B **22**, 5142 (1980).
[35]K. L. Chopra, *Thin Film Phenomena* (McGraw-Hill, New York, 1969), p. 344.
[36]G. Bergmann, Phys. Rev. Lett. **57**, 1460 (1986).
[37]P. R. Bevington, *Data Reduction and Error Analysis for the Physical Sciences* (McGraw-Hill, New York, 1986).
[38]R. W. Daniels, *An Introduction to Numerical Methods and Optimization Techniques* (North-Holland, Amsterdam, 1978).
[39]F. Komori, S. Kobayashi, and W. Sasaki, J. Phys. Soc. Jpn. **52**, 368 (1983).
[40]A. Abrikosov and L. P. Gorkov, Zh. Eksp. Theor. Fiz. **42**,

1088 (1962) [Sov. Phys. JETP **15**, 752 (1962)].
[41]J. Rammer and A. Schmid, Phys. Rev. B **34**, 1352 (1986).
[42]B. L. Altshuler, A. G. Aronov, and D. E. Khmel'nitskii, J. Phys. C **15**, 7367 (1982).
[43]W. E. Eiler, J. Low Temp. Phys. **56**, 481 (1984).
[44]R. P. Peters, G. Bergmann, and R. M. Mueller, Phys. Rev. Lett. **60**, 1093 (1988); W. Wei, R. Rosenbaum, and G. Bergmann, Phys. Rev. B **39**, 4568 (1989).
[45]J. C. Levy and J. L. Motchane, J. Vac. Sci. Technol. **9**, 721 (1972); G. Bayreuther, J. Magn. Magn. Mater. **38**, 273 (1983).
[46]M. Ben-Shlomo and R. Rosenbaum, Phys. Rev. B **39**, 534 (1989).